ELSEVIER

Surface Science 376 (1997) 69–76

surface science

Electrical conduction through the surface-state band of the Si(111)-$\sqrt{21} \times \sqrt{21}$-(Ag + Au) structure

Chun-Sheng Jiang [1], Xiao Tong, Shuji Hasegawa *, Shozo Ino

Department of Physics, School of Science, University of Tokyo, Hongo, Bunkyo-ku, Tokyo 113, Japan

Received 31 May 1996; accepted for publication 29 November 1996

Abstract

The Si(111)-$\sqrt{21} \times \sqrt{21}$ superstructure, which was induced by 0.14 atomic layer Au adsorption onto the Si(111)-$\sqrt{3} \times \sqrt{3}$-Ag surface at room temperature, was found to have a very high surface electrical conductance, higher than that of the Si(111)-7 × 7 clean surface by about 3.1×10^{-4} A/V. Photoemission spectroscopies showed that this $\sqrt{21}$ structure had a dispersive surface-state band crossing the Fermi level, while the surface space-charge layer was a depletion layer. It was thus concluded that the observed excess surface conductance was due to the two-dimensional band of the surface electronic state. © 1997 Elsevier Science B.V. All rights reserved.

Keywords: Angle-resolved photoemission spectroscopy; Reflection high-energy electron diffraction (RHEED); Silicon; Surface electrical transport; Surface electronic phenomena; Surface structure; X-ray photoelectron spectroscopy

1. Introduction

Electrical conduction near semiconductor surfaces is in general classified into three types, each of which is in principle closely related to the surface structure [1]:

(1) Conduction via a surface space-charge layer. Excess charges trapped in the surface state cause band bending below it, resulting in changes of carrier concentrations in the surface space-charge layer, whose width reaches several microns in a lightly doped semiconductor substrate. The surface electronic states of each superstructure thus can decisively govern the electrical conductivity through the layer.

(2) Conduction via surface-state bands. Two-dimensional bands are formed due to the surface superstructure. The electrons in the bands should be mobile along the surface just like electrons in the three-dimensional bulk bands, so that they contribute to electrical conduction. Conductivity of this type is directly dependent on the nature of the surface-state band (metallic or semiconducting) and also on the mobility of the carriers therein.

(3) Conduction via a grown atomic layer. If, for example, a metal atomic layer grows on a semiconductor surface at low temperatures, the grown layer dominates the conduction above a percolation-threshold coverage. Diffusivity of carrier scattering at surface/interface varies depending on the morphology of the surface, leading to changes of carrier mobility. So the growth modes and kinetics,

*Corresponding author. Fax: +81 3 5689 7257; e-mail: shuji@phys.s.u-tokyo.ac.jp.

[1] Present address: Surface and Interface Laboratory, The Institute of Physical and Chemical Research, Wako, Saitama 351-01, Japan.

0039-6028/97/$17.00 Copyright © 1997 Elsevier Science B.V. All rights reserved
PII S0039-6028(96)01569-5

which are dependent on the surface structure, sensitively affect the conductivity.

We have investigated the changes in surface electrical conductance during metal depositions onto the Si(111) substrate with various kinds of surface superstructures, and have found the crucial effects of the structure on the conductance [2]. However their mechanism has not yet been sufficiently clarified; the contributions of the conduction through the surface space-charge layer and the surface-state band are not clearly separated at the ranges of very low metal coverages where the metal-layer conduction is not yet set on.

In this paper we report measurements of the changes in electrical conductance combined with RHEED (reflection high-energy electron diffraction) observations and photoemission spectroscopies (angle-resolved ultraviolet and X-ray photoelectron spectroscopies, ARUPS and XPS) during Au deposition onto the Si(111)-$\sqrt{3}\times\sqrt{3}$-Ag surface at room temperature (RT). The structural changes during this deposition were as follows: a new superstructure of $\sqrt{21}\times\sqrt{21}$ appeared around 0.14 ML (monolayer) Au coverage [3,4], and with further deposition of Au, the surface changed into another $\sqrt{3}\times\sqrt{3}$ superstructure around 0.28 ML coverage. The surface electrical conductance drastically changed during this process; only the $\sqrt{21}\times\sqrt{21}$ phase had a much higher conductance compared with the initial and the other $\sqrt{3}\times\sqrt{3}$ phases. The ARUPS measurements showed that only the $\sqrt{21}$ structure had a dispersive surface-state band crossing the Fermi level (E_F), while the surface band bending measured by XPS showed that the surface space-charge layer tended to be a depletion layer under the $\sqrt{21}$ structure. Since Au of 0.14 ML is below the threshold coverage to make percolation paths, we have concluded that the drastic increase in surface conductance with formation of the $\sqrt{21}\times\sqrt{21}$ phase is due to electrical conduction through the newly formed two-dimensional surface-state band. This is the first report to confirm surface-state band conduction.

2. Experimental

A Si(111) wafer (p-type, resistivity = 20 Ω·cm) with a size of $20\times4\times0.4\ mm^3$ was cleaned by 1200°C flashings and annealing around 750°C with passing direct currents through the wafer. The $\sqrt{3}\times\sqrt{3}$-Ag structure was prepared at the substrate temperature of 510°C by Ag deposition with a rate of 0.4 ML/min. Deposition amounts of Ag and Au were calibrated with references of 1 ML Ag for completing the $\sqrt{3}\times\sqrt{3}$-Ag phase and 0.5 ML for the 5×2-Au phase, respectively. For the conductance measurements by a four-probe method with DC currents in ultra-high vacuum (UHV, in the 10^{-10} Torr range), we used a similar sample holder as in previous reports [2]. We confirmed the electrical contact conditions between the substrate and the Ta electrodes by observing a linear relation between the voltage signals and electrical currents. Sometimes, before cleaning the surface, the relation failed from linear. But after the cleaning by flashing several times, a good linear relation was observed. After the sample was cooled down to RT, Au was deposited onto the $\sqrt{3}\times\sqrt{3}$-Ag surface from a tungsten evaporator. Simultaneously, changes in conductance were measured by picking up the voltage signal between the inner pair of Ta-wire contacts, whose distance was about 10.2 mm, with a DC electric current of e.g. 70 μA supplied through the outer pair of Ta clamps.

To observe the changes of atomic structure, RHEED patterns were also monitored intermittently in situ during the metal depositions. Furthermore, to measure ARUPS and XPS, the Au deposition was interrupted, and the sample was transferred to another position in the same UHV chamber where a set of ARUPS and XPS apparatus (VG-ADES-500) worked. An angle-resolved analyzer was employed, which was a hemispherical type, rotating around two axes centered at the sample. An unpolarized He I (21.22 eV) light and a characteristic X-ray of Mg K_α (1253.6 eV) were used for the photoelectron excitations.

3. Results and discussion

Fig. 1 shows the RHEED pattern successively taken during Au deposition onto the $\sqrt{3}\times\sqrt{3}$-Ag surface at RT. The pattern began to change from the initial $\sqrt{3}\times\sqrt{3}$-Ag (Fig. 1a) to a

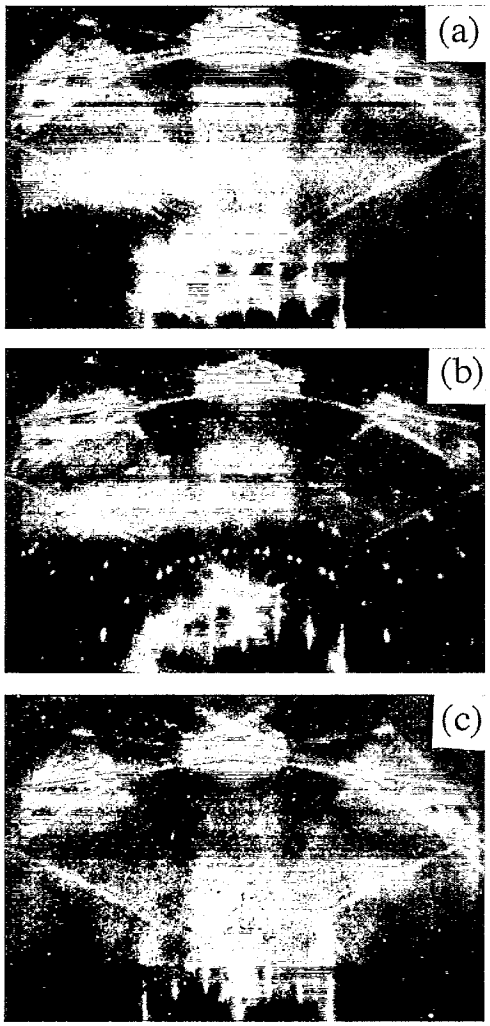

Fig. 1. RHEED patterns taken during Au deposition onto the Si(111)-$\sqrt{3}\times\sqrt{3}$-Ag surface at room temperature with the electron beam in [$2\bar{1}\bar{1}$] incidence. (a) The initial $\sqrt{3}\times\sqrt{3}$-Ag surface before Au deposition; (b) the $\sqrt{21}\times\sqrt{21}$ surface induced by adsorption of 0.14 ML Au; and (c) the $\sqrt{3}\times\sqrt{3}$-(Ag+Au) surface after 0.5 ML Au deposition.

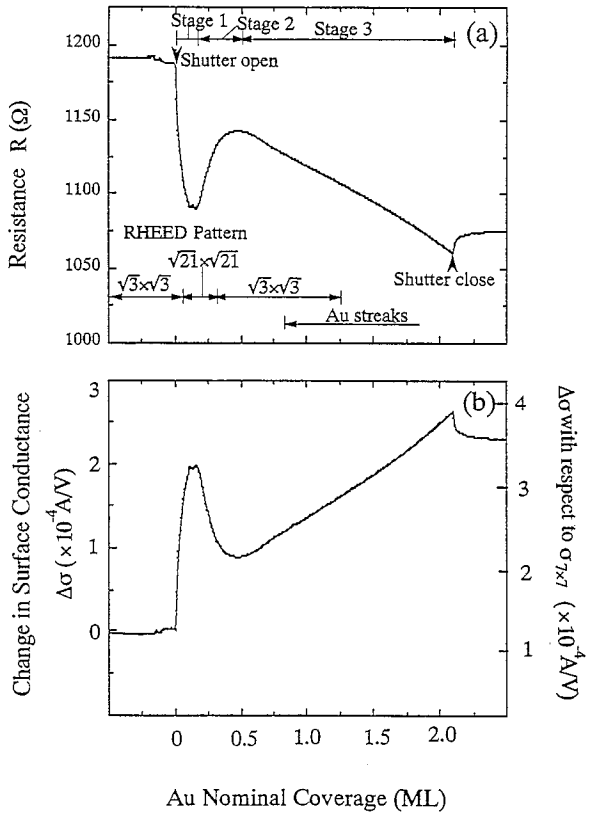

Fig. 2. (a) The change in resistance of the Si wafer during Au deposition onto the Si(111)-$\sqrt{3}\times\sqrt{3}$-Ag surface at room temperature with a deposition rate of 0.14 ML/min. (b) The change in electrical conductance during this deposition. This was calculated using the data of the resistance change shown in (a). The left-hand ordinate shows the conductance increase from the initial $\sqrt{3}$ surface, while the right-hand ordinate indicates the conductance increase with respect to the clean 7×7 surface.

$\sqrt{21}\times\sqrt{21}$-(Ag+Au) structure from 0.04 ML Au coverage, and the $\sqrt{21}$ spots gained maximum intensity around 0.14 ML deposition (Fig. 1b). With increasing the Au coverage further, the pattern returned to a $\sqrt{3}\times\sqrt{3}$-(Ag+Au) structure around 0.28 ML (Fig. 1c). The intensity distribution of this $\sqrt{3}\times\sqrt{3}$-(Ag+Au) pattern, however, was different from that of the initial $\sqrt{3}\times\sqrt{3}$-Ag (Fig. 1a); the (1/3,1/3) spots were stronger than (2/3,2/3) spots, while the initial $\sqrt{3}\times\sqrt{3}$ pattern had the opposite relative intensity. This means different atomic arrangements in their unit cells in spite of the same periodicity [4]. Streaks and halos emerged on this $\sqrt{3}\times\sqrt{3}$-(Ag+Au) pattern from 0.65 ML Au coverage. This $\sqrt{3}\times\sqrt{3}$ pattern vanished around 1.2 ML deposition.

Fig. 2a shows the change in resistance of the Si wafer during this Au deposition onto the Si(111)-$\sqrt{3}\times\sqrt{3}$-Ag surface at RT. When the evaporator shutter was opened, the resistance decreased

steeply by about −8.5% at first (up to ~0.14 ML coverage, stage 1), and then rose back up to about −4% (0.14 to ~0.5 ML coverage, stage 2). From 0.5 ML, it began to decrease slowly again until the deposition was stopped (more than 0.5 ML coverage, stage 3). With changing the Au deposition rate in a range of 0.054 to ~0.77 ML/min, no significant effect was observed; the amounts of resistance drop in stage 1 were almost the same within about 10% accuracy. The observed resistance drop in stage 1 corresponded precisely to the emergence of the $\sqrt{21}\times\sqrt{21}$ superstructure. The resistance rise in stage 2 corresponded to the disappearance of the $\sqrt{21}$ phase followed by conversion into the other $\sqrt{3}$ phase. Stage 3 corresponded to the degradation of the $\sqrt{3}$ phase.

Fig. 2b shows the conductance change $\Delta\sigma$ which was calculated from the resistance data in Fig. 2a; $\Delta\sigma=(1/R-1/R_0)(L/W)$, where R is the resistance at each Au coverage, R_0 is the resistance of the initial $\sqrt{3}\times\sqrt{3}$-Ag surface before Au deposition, L and W are the length and width of the measured area on the Si wafer, 10.2 and 4.0 mm, respectively. From the maximum $\Delta\sigma$ around 0.14 ML Au coverage, the surface conductance of the $\sqrt{21}$ phase is determined to be larger by 2.0×10^{-4} A/V than that of the initial $\sqrt{3}\times\sqrt{3}$-Ag surface $\sigma_{\sqrt{21}\times\sqrt{21}}$. In our previous paper [5], we have determined that $\sigma_{\sqrt{3}\times\sqrt{3}}$ is larger by 1.1×10^{-4} A/V than the surface conductance of the clean 7×7 phase $\sigma_{7\times7}$. Then, σ is larger than $\sigma_{7\times7}$ by 3.1×10^{-4} A/V.

When the Au deposition was interrupted at any time in the course of a resistance measurement like that of Fig. 2a, any significant changes in resistance as well as in the RHEED pattern were scarcely observed at these interruption periods. We then measured the Si 2p core-level shifts by XPS and valence-band states near E_F by UPS during these interruption periods as a function of Au coverage. It was found that the Si 2p core level shifted to larger binding energies compared with that at the initial $\sqrt{3}\times\sqrt{3}$-Ag surface by Au depositions up to around 0.15 ML where the $\sqrt{21}$ phase appeared. Then the peak shifted slightly to smaller binding energies with further Au deposition. In order to confirm the negligible effect of charging-up in photoemission spectroscopy, we changed the input power of the X-ray tube to double the X-ray intensity. Evaluation of the changes in band bending relies on the data of the Si 2p core-level shifts in XPS. This is because the energy of the emitted photoelectrons from the Si 2p level is so high (higher than 1 keV) that our XPS measurements are bulk sensitive, not surface sensitive, so that it is insensitive to any surface chemical shifts. Therefore the data of the Si 2p core-level shifts can be used to evaluate plausible surface E_F shifts as in Fig. 3a. Here, we adopted the E_F position at the initial $\sqrt{3}\times\sqrt{3}$-Ag surface to be at 0.1 eV above the valence-band maximum (VBM) [6], which means its surface space-charge layer is a hole-accumulation layer. Then, it can be said that the E_F shifted from the initial position near the VBM to the bulk E_F position with less than 0.1 ML Au adsorption. This leads to a conversion of the surface space-charge layer from a hole-accumulation condition to a flat-band condition, which corresponded to the emergence of the $\sqrt{21}$ phase. With further deposition beyond saturation coverage of the $\sqrt{21}$ phase, the E_F returns slightly towards the VBM, but not near enough to the VBM to return to the hole-accumulation condition.

From the resistivity of our Si wafer, the E_F position in the bulk can be estimated to be 0.29 eV above the VBM. Then, if the E_F position at the surface is given, the electric field (band bending), the excess carrier concentration, and the resulting excess conductance in the surface space-charge layer can be calculated by solving the Poisson equation [7]. The solid curve in Fig. 3b shows the calculated excess surface conductance through the space-charge layer as a function of the surface E_F position. When the surface E_F is located near the VBM or the conduction-band minimum, the electrical conductance should be enhanced because of the accumulations of excess holes or electrons in the surface space-charge layer, respectively. When, on the other hand, the surface E_F lies around the middle of the band gap, the excess carriers are depleted, so that electrical conductance through the surface space-charge layer should be lowered. By tracing the observed shifts of the surface E_F position in Fig. 3a on this graph, from 0.1 to 0.3 eV above the VBM, it is found that the

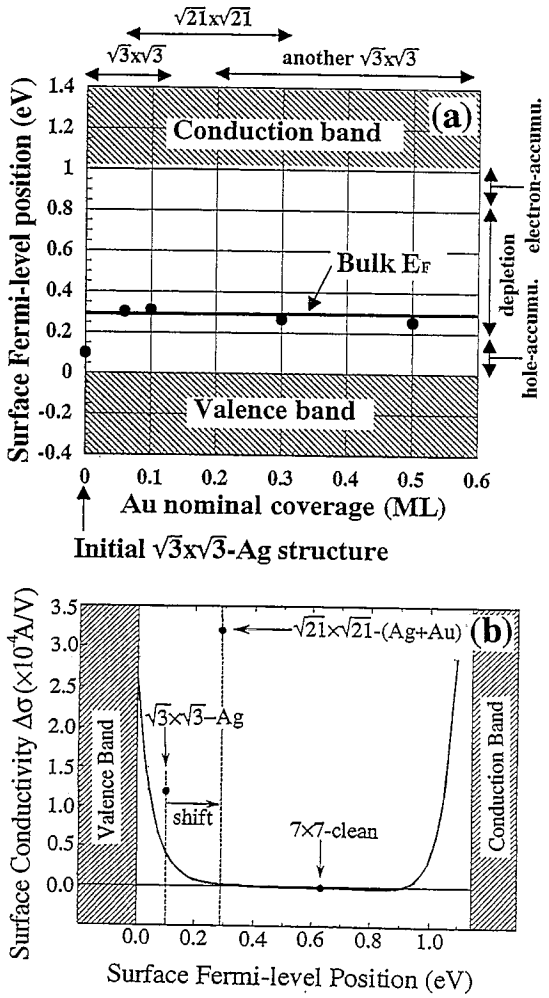

Fig. 3. (a) The shifts of the surface Fermi-level position as a function of Au coverage. These were determined from the peak shifts of Si 2p core-level in XPS during Au deposition onto the Si(111)-$\sqrt{3}\times\sqrt{3}$-Ag surface at room temperature. The Fermi-level position at the initial $\sqrt{3}$ surface was taken to be 0.1 eV above the VBM according to Ref. [6]. (b) The excess electrical conductance through the surface space-charge layer as a function of the surface Fermi-level position, which was calculated by solving a Poisson equation using the values of the carrier mobilities in the bulk. The electrical conductance under the flat-band condition was defined as the reference. The measured increases in conductance at the $\sqrt{3}\times\sqrt{3}$-Ag and $\sqrt{21}\times\sqrt{21}$ surfaces compared with the clean 7×7 surface are also plotted at the respective surface E_F positions. Such data points are located above the calculated curve, which means some extra conductions in addition to those through the surface space-charge layer.

surface space-charge layer is converted from a hole-accumulated condition at the initial $\sqrt{3}\times\sqrt{3}$-Ag surface into a flat-band condition at the $\sqrt{21}\times\sqrt{21}$ phase where the excess holes are depleted. Then electrical conduction through the surface space-charge layer should be suppressed. By contrast, the measured surface conductance was greatly enhanced.

ARUPS spectra near E_F were measured over the surface Brillouin zone for the three different surfaces, the initial $\sqrt{3}\times\sqrt{3}$-Ag surface, the $\sqrt{21}\times\sqrt{21}$ structure at 0.14 ML Au coverage, and the other $\sqrt{3}\times\sqrt{3}$ phase at 0.5 ML Au coverage. For the initial $\sqrt{3}$ surface, no emission intensity at E_F was detected at any emission angles, as in the literature [8]. This means a semiconductor-like surface electronic structure at this surface. Figs. 4a and 4b show the spectra taken from the $\sqrt{21}$ surface. Though at normal emission, any significant intensity was not detected near E_F, at other emission angles, metallic edges immersing the E_F were observed. In particular, the peaks indicated by arrow heads appear at narrow ranges of angle, and seem to be dispersive across E_F. This clearly shows that the surface electronic state converted into a metallic one at the $\sqrt{21}$ phase from the semiconductor-like one at the initial $\sqrt{3}$ phase with the structural transformation. The nature of this surface-state band will be discussed in detail later.

Fig. 4c shows the ARUPS results measured from the $\sqrt{3}\times\sqrt{3}$ structure with 0.5 ML Au coverage which was prepared by further Au deposition onto the $\sqrt{21}$ structure. The spectra became featureless; the characteristic peaks observed in Fig. 4b for the $\sqrt{21}$ phase vanished. But weak metallic edges at E_F are observed at all emission angles in Fig. 4c, which come from three-dimensional metal islands formed with excess Au (and Ag) atoms. Au deposited onto the $\sqrt{21}$ surface will exchange their atomic positions with the underlying Ag atomic layer to destroy the $\sqrt{21}\times\sqrt{21}$ periodicity, and tend to make small metal islands [9]. These islands were observed by scanning tunnelling microscopy. Thus, it is concluded that the surface-state band crossing E_F in Fig. 4b disappears, and the surface electronic structure returns to a semiconductor-like one with the structural transition from the $\sqrt{21}\times\sqrt{21}$-(Ag+Au) to the $\sqrt{3}\times\sqrt{3}$-(Ag+Au) on

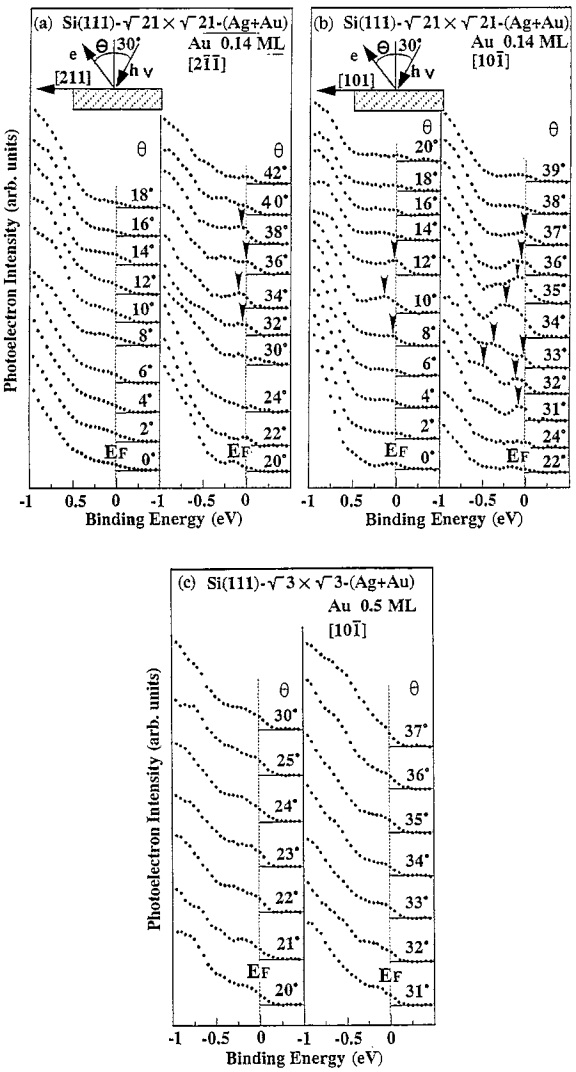

Fig. 4. Angle-resolved UPS spectra measured from (a), (b) the Si(111)-$\sqrt{21}\times\sqrt{21}$-(Ag+Au) surface with 0.14 ML Au coverage, and (c) the $\sqrt{3}\times\sqrt{3}$-(Ag+Au) surface with 0.5 ML Au coverage, scanned in (a) [2$\bar{1}\bar{1}$] and (b), (c) [10$\bar{1}$] directions. The angle of incidence of the ultra-violet light was set at 30° from the surface-normal direction.

increasing Au coverage. During this process, the band bending does not show any significant change in Fig. 3a. Therefore, the increase of resistance in stage 2 in Fig. 2a can be attributed to the effect of suppression of the dispersive surface-state band of the $\sqrt{21}$ phase.

Now, the origin of the very high surface conductance of the $\sqrt{21}\times\sqrt{21}$ phase can be clarified. Electrical conduction through the surface space-charge layer was excluded because of the opposite band bending as measured by XPS in Fig. 3. Au of 0.14 ML coverage is too small to make percolation paths on the two-dimensional triangular lattice [10]. So we have to conclude that the surface-state band crossing E_F in Figs. 4a and 4b enhances the electrical conductance of the $\sqrt{21}\times\sqrt{21}$ phase.

Next, we discuss the nature of the observed surface-state conduction. The initial $\sqrt{3}\times\sqrt{3}$-Ag surface, whose atomic structure is now solved as the honeycomb–chained trimer (HCT) model [11], is known to have a characteristic surface-state band, called the S_1-state band. This band is strongly upwards-dispersing, and its minimum is close to E_F at the $\bar{\Gamma}$ point in the surface Brillouin zone. These features are experimentally observed [12], and also reproduced by the first-principles calculations [13]. This is, however, not a metallic band. The surface electronic structure is inherently semiconductor-like. Our in-situ ARUPS measurements did not show any photoemission intensity at E_F over the Brillouin zone as in the literature [8], because the minimum of the S_1-state band is above E_F, so that not enough electrons are thermally excited into this surface-state band to give rise to the photoemission intensity. But the electrons in this band can contribute to electrical conduction parallel to the surface, because the S_1-state band is highly dispersive [5]. The surface charging, which is the origin of the upward band bending below the $\sqrt{3}\times\sqrt{3}$-Ag surface, is naturally understood by considering the excess electrons trapped in this S_1-state band [12,14]. So if the Au atoms deposited on top of the $\sqrt{3}\times\sqrt{3}$-Ag surface donate the excess electrons into the S_1-state band, conduction through this surface-state band will be enhanced. On the other hand, since the accumulation of excess electrons in the S_1-state should be in neutral balance with the positively charged Au atoms ("surface donor ions") on top of the $\sqrt{3}\times\sqrt{3}$ frame, the additional Au atoms will not cause the band bending to change. However, the observed change in band bending was actually downward (Fig. 3a). So this is not the case; this scenario of doping the excess electrons into the initial $\sqrt{3}\times\sqrt{3}$-Ag surface-state band is excluded as a

possible explanation of the high surface-state conductivity of the $\sqrt{21} \times \sqrt{21}$-(Ag+Au) phase. So we have to rely on the newly formed dispersive band observed in Figs. 4a and 4b. The symmetry of this band is different from that of the S_1-state band of the initial $\sqrt{3} \times \sqrt{3}$-Ag surface, though we could not confirm its $\sqrt{21} \times \sqrt{21}$ symmetry. Since the $\sqrt{21}$ phase has double domains rotating by 21.8° with respect to each other, it is not straightforward to map the band dispersion.

For the $\sqrt{21} \times \sqrt{21}$-(Ag+Au) structure, two different structural models are proposed by Nogami et al. [3] and Ichimiya et al. [4]. While the two models have different Au coverage on top of the initial $\sqrt{3} \times \sqrt{3}$-Ag surface, 0.19 ML and 0.14 ML, respectively, both have a common feature that the initial $\sqrt{3} \times \sqrt{3}$-Ag framework remains; a $\sqrt{21} \times \sqrt{21}$ periodicity is produced only with additional Au atoms. So the observed surface-state band of the $\sqrt{21} \times \sqrt{21}$ structure is considered to come inherently from delocalization of electrons of periodically arranged Au atoms. According to the model by Ichimiya et al., the deposited Au atoms sit on the center of Si trimers of the initial $\sqrt{3} \times \sqrt{3}$-Ag structure, while the model by Nogami et al. suggests an adsorption site for Au at the center of Ag trimers. In order to determine which model is consistent with our photoemission data for the $\sqrt{21}$-structure, and to characterize the surface-state band, some theoretical calculations are needed, based on a correct atomic model.

Scanning tunnelling microscopy (STM) reveals that atomic steps on a metal surface act as scattering centers for electrons in a surface-state band. This effect has been demonstrated as standing waves of electrons near the surface step edges [16,17]. Though this scattering effect is therefore considered to be important for the surface-state conductivity, we believe for the following reasons that the excess electrical conductance due to the surface-state band is still detectable by measurements even with a pair of macroscopically separated probes as reported in the present paper. Although the atomic steps and domain boundaries act as scattering centers for the carriers in the surface-state band, resulting in a reduction of their mobility, highly conductive surface areas in the respective domains of the $\sqrt{21}$ phase can actually lower the resistance averaged over the macroscopic distance, if the domains are large enough compared with the mean free path of the carriers. Furthermore, the significance of the scattering effect by steps may depend on the Fermi wavelength of the carriers which is determined by the carrier concentration. On metal surfaces used in the STM observations of the electron standing waves [16,17], the Fermi wavelength of the surface-state electrons is considered to be short because of its high concentration. But in our $\sqrt{21}$ phase, it is not necessarily the case, probably because of a much lower density of the carriers. Since, however, at the present stage, we can not quantitatively estimate the scattering effect from this viewpoint, this is an open question for future studies. We are now going to measure the mobility of the carriers in the surface-state band using the Hall effect.

It is worthy to note, lastly, that similar $\sqrt{21} \times \sqrt{21}$ structures appear on the Si(111)-$\sqrt{3} \times \sqrt{3}$-Ag surface not only by additional Au deposition at RT, but also by additional Cu deposition at RT [15], or by additional Ag deposition below 250 K [18,19]. We have found that all of these $\sqrt{21} \times \sqrt{21}$ phases are formed around 0.14 ML coverage of the additional metal, and that all show very high surface electrical conductance [19]. Common features in atomic and electronic structures among these three $\sqrt{21} \times \sqrt{21}$ structures were observed by our preliminary measurements of STM and photoemission spectroscopies. The details will be reported elsewhere.

Acknowledgements

We thank Prof. M. Henzler of Hannover University for his helpful discussions on the interpretation of our data. This work is supported by a Grant-In-Aid from the Ministry of Education, Science and Culture of Japan, and also by the Sumitomo Foundation.

References

[1] M. Henzler, in: Surface Physics of Materials I, Ed. J.M. Blakely (Academic Press, New York, 1975) p. 241.

[2] S. Hasegawa and S. Ino, Phys. Rev. Lett. 68 (1992) 1192; Surf. Sci. 283 (1993) 438; Thin Solid Films 228 (1993) 113; Int. J. Mod. Phys. B 7 (1993) 3817.
[3] J. Nogami, K.J. Wan and X.F. Lin, Surf. Sci. 306 (1994) 81.
[4] A. Ichimiya, H. Nomura, Y. Horio, T. Sato, T. Sueyoshi and M. Iwatsuki, Surf. Rev. Lett. 1 (1994) 1.
[5] C.S. Jiang, S. Hasegawa and S. Ino, Phys. Rev. B 54 (1996) 10389.
[6] S. Kono, K. Higashiyama, T. Kinoshita, T. Miyahara, H. Kato, H. Osawa, Y. Enta, F. Maeda and Y. Yaegashi, Phys. Rev. Lett. 58 (1987) 1555.
[7] C.E. Young, J. Appl. Phys. 32 (1961) 329.
[8] T. Yokotsuka, S. Kono, S. Suzuki and T. Sagawa, Surf. Sci. 127 (1983) 35.
[9] T. Yamanaka, A. Endo and S. Ino, Surf. Sci. 294 (1993) 53.
[10] R. Schad, S. Heun, T. Heidenblut and M. Henzler, Phys. Rev. B 45 (1992) 11430.
[11] T. Takahashi and S. Nakatani, Surf. Sci. 282 (1993) 17; Y.G. Ding, C.T. Chan and K.M. Ho, Phys. Rev. Lett. 67 (1991) 1454; S. Watanabe, M. Aono and M. Tsukada, Phys. Rev. B 44 (1991) 8330.
[12] L.S.O. Johansson, E. Landemark, C.J. Karlsson and R.I.G. Uhrberg, Phys. Rev. Lett. 63 (1989) 2092.
[13] Y.G. Ding, C.T. Chan and K.M. Ho, Phys. Rev. Lett. 69 (1992) 2452.
[14] L.S.O. Johansson, E. Landemark, C.J. Karlsson and R.I.G. Uhrberg, Phys. Rev. Lett. 69 (1992) 2451.
[15] I. Homma, Y. Tanishiro and K. Yagi, in: The Structure of Surfaces III, Eds. S.-Y. Tong et al. (Springer, Berlin, 1991) p. 610.
[16] Y. Hasegawa and Ph. Avouris, Phys. Rev. Lett. 71 (1993) 1071.
[17] M.F. Crommie, C.P. Lutz and D.M. Eigler, Nature 363 (1993) 524.
[18] Z.H. Zhang, S. Hasegawa and S. Ino, Phys. Rev. B 52 (1995) 10760.
[19] X. Tong, S. Hasegawa and S. Ino, Phys. Rev. B 55 (1997) 1310.